PERFORMANCE ANALYSES OF 10MW COMPOSITE WIND-TURBINE BLADE CONSIDERING AEROELASTIC EFFECTS

D.H. Kim[1*], Y.H. Kim[1], and S.H. Kim[2]
[1] Department of Aerospace and System Engineering, Gyeongsang National University (GNU), Jinju City, South Korea, [2] CAE-Korea Co., Ltd., Jinju City, South Korea
* Corresponding author (dhk@gnu.ac.kr)

Keywords: *Wind-Turbine, Composite Blade, Aeroelastic Response, Fluid-Structure Interaction*

1 Introduction

The current technical trend in the development of wind turbine system shows a vast increase in turbine dimensions. Because the power captured by wind turbines is directly proportional to the square of the rotor diameter. In addition, the trend for current wind turbine development is to go offshore, where wind turbines have a higher energy potential because of the higher wind speeds. Due to the combination of high wind speeds and large size of the turbines, tremendous loads are caused in the rotating turbine blade structures. Therefore, accurate aeroelastic analysis system for large wind turbine blade is important to investigate the operational stability of designed wind turbine blades. Also, there are several previous researches about flutter analyses of wind turbine blade systems [1-6].

Generally, wind turbine systems consist of rotor blade, hub, generator, and gear box etc., and the wind turbine system are defined as HAWT (Horizontal Axis Wind Turbine) and VAWT (Vertical Axis Wind Turbine). Recently, MW-class huge wind-turbines are designed as HAWT type with three-blades constructed by advanced composite materials.

In the case of flutter the oscillatory motion of the blade necessitates the use of unsteady aerodynamic loads. In this study, to obtain numerical results for blade aerodynamic loads with sufficient quality, Reynolds-averaged Navier-Stokes (RANS) equations are applied with an appropriate fine grid mesh in the computational domain. Multi-body dynamic analyses of rotating wind-turbine blade have been conducted using the general nonlinear finite element program, MSC/NASTRAN and SAMCEF. Advanced coupled aeroelastic analysis system based on computational fluid dynamics (CFD) and computational multi-body dynamics (CMBD) has been developed in order to investigate detailed aeroelastic responses and flutter stability of general wind-turbine blade configurations. Especially, effects of rotation and flow separation with respect to the rotating and vibrating blade are considered in numerical analyses. Fluid domains are modeled using the unstructured grid system with dynamic moving and local deforming techniques. Unsteady, Reynolds-averaged Navier-Stokes equations with k-εturbulence models using FLUENT and developed user-defined function (UDF) codes are solved for unsteady flow problems with blade rotation and deformation effects. A fully implicit time marching scheme based on the Newmark time-integration method is typically used for computing the coupled aeroelastic governing equations of the rotating blade fluid-structure interaction problems. Fluid-structure coupling algorithms and main integration code including required various sub-modules have been successfully developed in this study. Practical program module (FSIPRO3D) developed by CAE-KOREA Inc. can be applied to general fluid-structure interaction problems. This FSI analysis system was verified using AGARD 445.6 wing what is famous for verifying the flutter analysis method because that has experiment data [7].

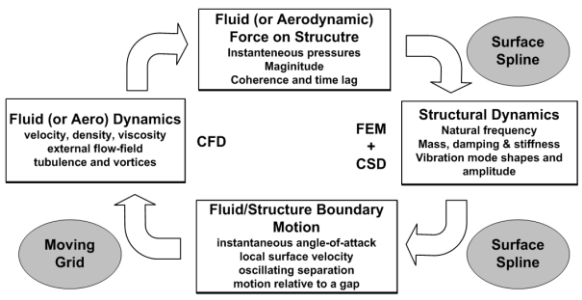

Fig. 1. Aeroelastic engineering feedback mechanism between fluid and structure domains.

It shows FSIPRO3D can effectively combine FLUENT software and any kind of commercial finite element software such as SAMCEF, MSC/NASTRAN, ABAQUS, and ANSYS etc. for the general applications of FSI problems. In order to conduct accurate aeroelastic response analysis engineering feedback mechanism (Fig.1.) is fully considered in the present coupled computational analysis process.

For numerical results, aeroelastic response analyses of a 10 MW wind turbine blade of 82.18 m length are considered herein. The results for aerodynamic, vibration and aeroelastic analyses are presented in detail.

2 Computational Backgrounds

2.1 Unsteady Aerodynamic Model

Unsteady compressible RANS equations can be given as tensor form by

$$\frac{\partial \rho}{\partial t} + \frac{\partial}{\partial t}(\rho u_i) = 0 \tag{1}$$

$$\frac{\partial}{\partial t}(\rho u_i) + \frac{\partial}{\partial x_i}(\rho u_i \tilde{u}) = -\frac{\partial p}{\partial x_i} + \frac{\partial}{\partial x_j}[\tau_{ij} + R_{ij}] \tag{2}$$

where the viscous stress tensor and deformation tensor are defined as

$$\tau_{ij} = 2\mu[S_{ij} - \frac{1}{3}\delta_{ij}\frac{\partial u_k}{\partial x_k}]$$

$$S_{ij} = \frac{1}{2}[\frac{\partial u_i}{\partial x_j} + \frac{\partial u_j}{\partial x_i}]$$

Also,

$$\tilde{u} = u_j - u_{g,j}$$

where $u_{g,j}$ is the grid velocity. And turbulence Reynolds stress tensor R_{ij} must be modeled in order to close Eq.(2). This tensor may be approximated by Following Boussinesq hypothesis:

$$R_{ij} \cong \mu_T[S_{ij} - \frac{2}{3}\frac{\partial u_k}{\partial x_k}\delta_{ij}] - \frac{2}{3}(\rho k)\delta_{ij} \tag{3}$$

In this study, Eqs.(1)~(3) are solved by using the FLUENT software based on the finite-volume method. Also, aeroelastic coupling program written by C language is originally developed based on the user defined function (UDF) of FLUENT software in order to be coupled with structural equations in the modal domain. In this study, the implicit coupled solver and the two-equation k-ε turbulence model are used. For the discretization of RANS equations, second-order upwind scheme is applied.

In this study, standard k-ε turbulence model[4] was used. The standard k-ε model is a semi-empirical model based on model transport equations for the turbulence kinetic energy (k) and its dissipation rate (ε). The model transport equation for k is derived from the exact equation, while the model transport equation for εwas obtained using physical reasoning and bears little resemblance to its mathematically exact counterpart.

In the derivation of the k-ε model, the assumption is that the flow is fully turbulent, and the effects of molecular viscosity are negligible. The standard k-ε model is therefore valid only for fully turbulent flows.

The turbulence kinetic energy and its rate of dissipation are obtained from the following transport equations:

$$\frac{\partial}{\partial t}(\rho k) + \frac{\partial}{\partial x_i}(\rho k u_i) = \frac{\partial}{\partial x_j}\left[\left(\mu + \frac{\mu_t}{\sigma_k}\right)\frac{\partial k}{\partial x_j}\right] + G_k + G_b - \rho\varepsilon - Y_M + S_k$$

and,

$$\frac{\partial}{\partial t}(\rho \varepsilon) + \frac{\partial}{\partial x_i}(\rho \varepsilon u_i) = \frac{\partial}{\partial x_j}\left[\left(\mu + \frac{\mu_t}{\sigma_\varepsilon}\right)\frac{\partial k}{\partial x_j}\right] + C_{1\varepsilon}\frac{\varepsilon}{k}\left(G_k + C_{3\varepsilon}G_b\right) - C_{2\varepsilon}\rho\frac{\varepsilon^2}{k} + S_\varepsilon$$

In these equations, G_k represents the generation of turbulence kinetic energy due to the mean velocity gradients, G_b is the generation of turbulence kinetic energy due to buoyancy, Y_M represents the contribution of the fluctuating dilatation in compressible turbulence to the overall dissipation rate, $C_{1\varepsilon}$, $C_{2\varepsilon}$, and $C_{3\varepsilon}$ are constants. σ_k and σ_ε are the turbulent Prandtl numbers for k and ε, respectively. S_k and S_ε are user-defined source terms.

The model constants $C_{1\varepsilon}$, $C_{2\varepsilon}$, C_μ , σ_k and σ_ε have the following default values:

$$C_{1\varepsilon} = 1.44,\ C_{2\varepsilon} = 1.92,\ C_\mu = 0.09,$$
$$\sigma_k = 1.0,\ \sigma_\varepsilon = 1.3.$$

The turbulent (or eddy) viscosity, μ_t , is computed by combining k and ε as follows:

$$\mu_t = \rho C_\mu \frac{k^2}{\varepsilon}$$

2.2 Aeroelastic Model with Rotating Effect

The governing aeroelastic equations of motion of a flexible blade can be obtained by using the Rayleigh-Ritz method. In this method, the resulting aeroelastic displacement at any time can be expressed as a function of a finite set of selected modes. The general motion of the blade can be described by the separation of time and space variables as follows:

$$\begin{aligned} \{u(t)\} &= [\Psi_x(x,y,z,\omega)]\{q(t)\} \\ \{v(t)\} &= [\Psi_y(x,y,z,\omega)]\{q(t)\} \\ \{w(t)\} &= [\Psi_z(x,y,z,\omega)]\{q(t)\} \end{aligned} \tag{4}$$

where $\{u(t)\}$, $\{v(t)\}$ and $\{w(t)\}$ are the time-dependent structural deflections and $[\psi_x]$, $[\psi_y]$ and $[\psi_z]$ are the matrices of x-, y-, z-direction displacements of the natural vibration modes and those are the function of rotation speed. The aeroelastic governing equations of motion for an elastic wing are formulated in terms of generalized displacement response vector $\{q(t)\}$ which is a solution of the following equation:

$$\begin{aligned} &[M_g(\omega)]\{\ddot{q}(t)\} + [C_g(\omega)]\{\dot{q}(t)\} + [K_g(\omega)]\{q(t)\} \\ &= \{F_g(t,q,\dot{q},\omega)\} \end{aligned} \tag{5}$$

where t is the physical time, $[M_g]$ is the generalized mass matrix, $[C_g]$ is the generalized damping matrix, $[K_g]$ is the generalized stiffness matrix, and $\{F_g\}$ is the vector of generalized aerodynamic forces computed by integrating the pressure distributions on the wing surface as

$$F_{g_i} = \frac{1}{2}\rho U^2 c_r^{\,2} \iint_S -Cp(x,y,z,\omega,t)\left(n_x\psi_{xi} + n_y\psi_{yi} + n_z\psi_{zi}\right)\frac{dS}{c_r^{\,2}} \tag{6}$$

where ρ is the free stream air density, U is the free stream velocity, c_r is the reference chord length, S is the wing area, C_p is the instantaneous unsteady pressure coefficient on the arbitrary blade surface, n_x, n_y, and n_z mean the surface normal vectors for x, y and z direction, respectively and ψ_i are the i-th natural mode shape vectors interpolated on the aerodynamic surface mesh. The generalized aerodynamic forces of Eq. (6) are integrated numerically on the blade surfaces. In this study, the coupled time-marching method is used to effectively investigate characteristics of nonlinear aeroelastic responses of rotating blade systems in detail. The time marching process of the structure-fluid coupling is performed by similarly adopting the second-order staggered algorithm. The computational process for the present coupling process applied in this study is shown in Fig. 2. More detailed theoretical description and applications for the present computational method can be found in Refs.6-8.

$$\{q(t)\}^T = [q(t)_1, q(t)_2, q(t)_3 \cdots, q(t)_m]$$
$$[M_g(\omega)] = [\phi(\omega)]^T[M][\phi(\omega)]$$
$$[C_g(\omega)] = [\phi(\omega)]^T[C][\phi(\omega)]$$
$$[K_g(\omega)] = [\phi(\omega)]^T[K(\omega)][\phi(\omega)]$$
$$\{Q(t,q,\dot{q},\omega)\} = [\phi(\omega)]^T\{F(t,u,\dot{u},\omega)\}$$

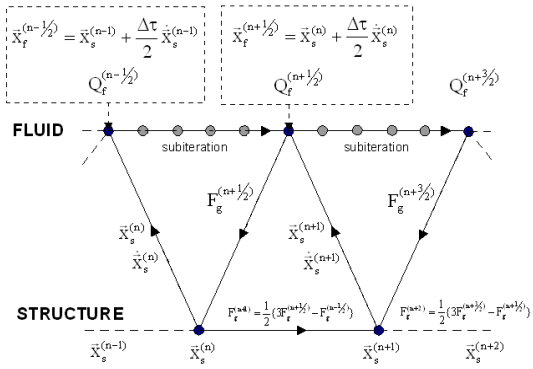

Fig.2. Fluid-structure coupled computational process using the second-order time-accurate staggered method.

3 Results and Discussion

In this study, the performance analyses of a 10MW class wind-turbine composite blade model have been performed using an advanced computational approach with FSIPRO3D. The diameter of rotor is 164 m and the length of blade is 82.18 m. The blade is composed of upper skin, lower skin, spar cab, shears web and bonding parts.

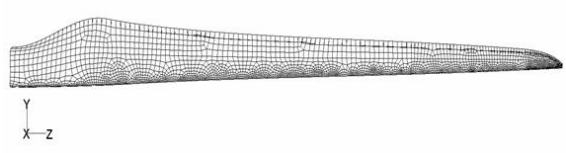

(a) Computational surface grid

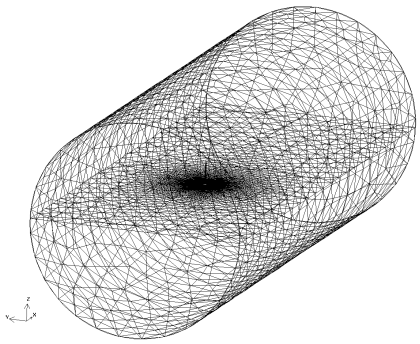

(b) Computational domain grid

Fig.3. CFD grid of 10MW turbine blade.

The generated fluid domain grid of the MW-class blade is presented in Fig.3. The total number of volume is about 117,311. The fluid condition at sea level altitude with 9 m/s, 8 RPM and 13 m/s, 12 RPM is considered. Multiple Rotating Frames (MRF) method is effectively applied to consider rotating motion of the blade and k-ε turbulence model is applied to consider flow viscosity effects of the blade.

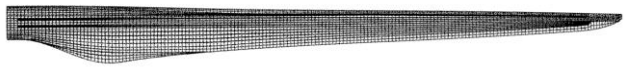

(a) Whole blade

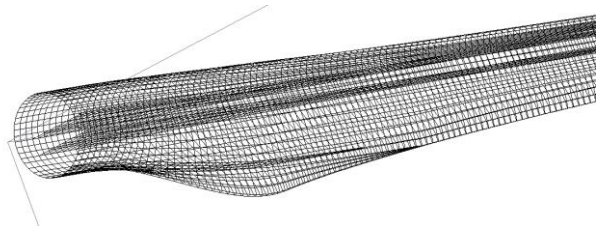

(b) Closed view

Fig.4. Finite element model for the present laminated composite blade.

Table.1. Material properties for composite blade.

UD				
E11(GPa)	E22(GPa)	G12(GPa)	ν12	ρ(kg/m3)
43.1	13.2	3.62	0.241	1,939
S1T(MPa)	S2T(MPa)	S1C(MPa)	S2C(MPa)	SS(MPa)
916	41	759	124	38

Balsa		
E(GPa)	ν	ρ(kg/m3)
3.72	0.1	151

For aeroelastic simulations, structural finite element model for a 10 MW-class wind turbine rotor was constructed as using quadrilateral plate element. For simplicity, the wind-turbine structural model was assumed as shell structure as presented in Fig.4. and the total number of structural nodes is 8,894. Materials of laminated composite blade are presented in Table.1 The rotating speed was applied to the structure and the root section was clamped to impose structural boundary condition.

Calculated natural frequencies are presented in Table 2 and natural vibration mode shapes are

presented in Fig.5. The results typically show that the 1st eigenmode is the fundamental flapwise bending mode. The 2nd eigenmode is 1st edgewise bending mode. The 3rd mode looks like the 2nd flapwise bending mode. The 4th mode corresponds to 2nd edgewise bending mode.

Table.2. Material properties for composite blade.

RPM	1st mode	2nd mode	3rd mode	4th mode
8	0.74	1.14	2.22	3.85
13	0376	1.15	2.25	3.87

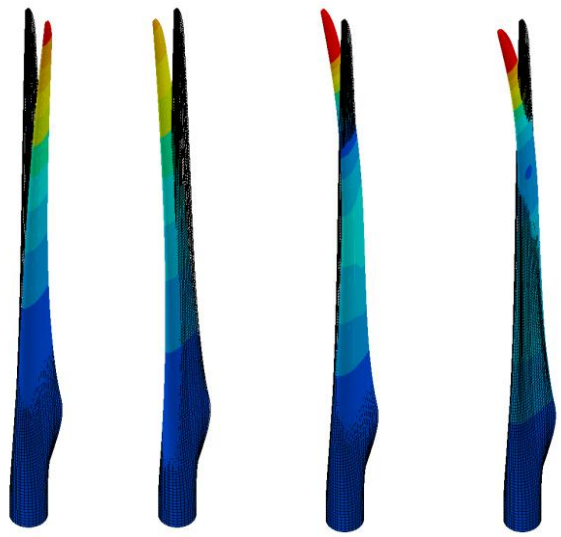

Mode1 Flapwise bending | Mode2 Edgewise Bending | Mode3 2nd flapwise bending | Mode4 2nd edgewise bending

Fig.5. Natural vibration mode shapes and frequencies.

Fig.6 shows the comparison results for the power of 10 MW wind turbine blade between the rigid and the flexible models with 9 m/s and 13 m/s. It is importantly shown that estimated generation power can be significantly different due to the effect of aeroelastic deformation. This means that the designed data for blade control logic also need to be modified considering important aeroelastic effects for large blade. We can expect that the much larger blade can show the much different effect.

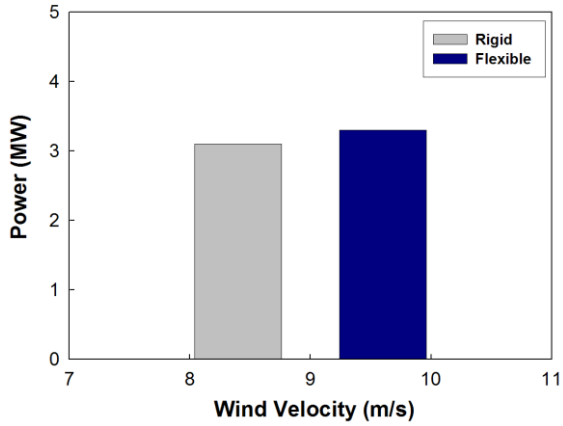

(a) U = 9 m/s

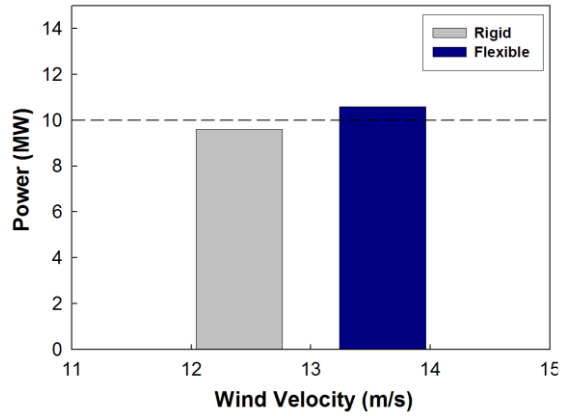

(b) U = 13 m/s

Fig.6. Comparison of aerodynamic power between the rigid and the flexible blade models.

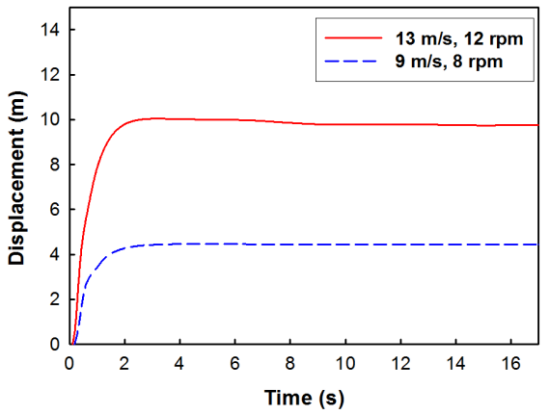

(a) x-direction

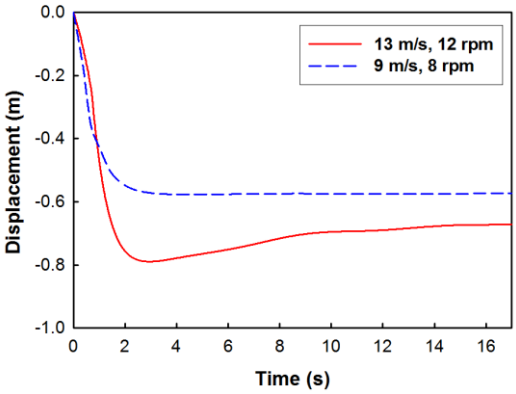

(b) y-direction

Fig.7. Aeroelastic displacement responses.

The results for time-domain aeroelastic response analysis are presented in Fig.7. The aeroelastic responses are maximum displacement of the blade.

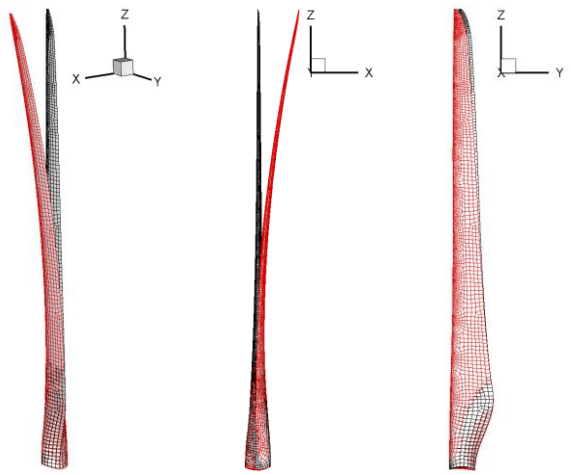

Isoperimetric view | X-Z plane view | Y-Z plane view

Fig.8. Instantaneous aeroelastic deformation shapes.

Fig.8. shows the instantaneous aeroelastic deformed shape of rotating wind-turbine blade. It is shown that the total aeroelastic deformation is composed of the flapwise and edgewise bending deflections. Here, the bending deflection seems to be dominant. Fig.9. shows the comparison of instantaneous pressure contours with stream lines between rigid and elastic model. As can be expected, the instantaneous flow patterns show different characteristic due to aeroelastic deformation. This is the reason why the generated power for the rigid and the flexible blade model can be different for the same flow condition.

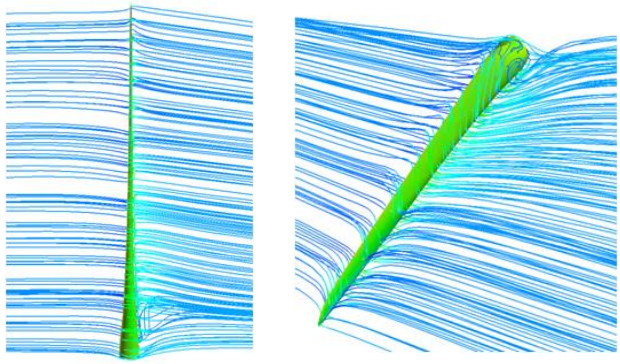

(a) Rigid blade model

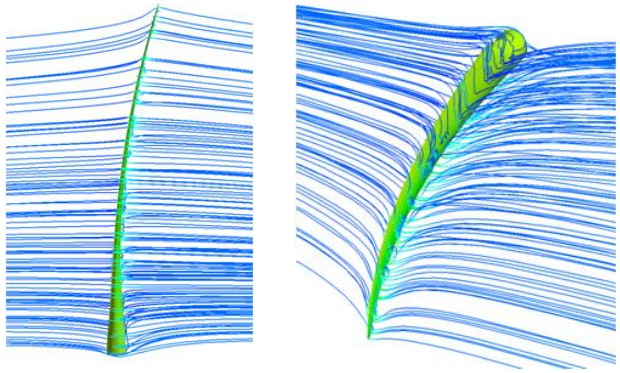

(b) Aeroelastic blade model

Fig.9. Comparison of instantaneous pressure contours with stream lines. (rigid vs elastic blade)

4 Conclusions

In this study, accurate performance analyses of a 10 MW class wind-turbine composite blade model have been successfully performed using an advanced computational approach using a general fluid-structure interaction analysis module (FSIPRO3D). It is importantly shown that the effect of aeroelastic behaviors play an important role in predicting both the load and the performance of the huge wind-turbine model. Considering this kind of accurate computational results for the design of wind-turbine and its controllers must be valuable in the actual design process for the guaranteed successful development of very huge wind-turbine systems.

References

[1] S. Streiner, E. Kramer, A. Eulitz, and P. Armbruster, “Aeroelastic Analysis of Wind Turbines Applying 3D CFD Computational Results”, Journal of Physics,

Conference series 75, 2007.

[2] A. Ahlstrom, “Aeroelastic Simulation of Wind Turbine Dynamics”, Doctoral Thesis from Royal Institute of Technology Department of Mechanics, Sweden, 2005.

[3] A. Ahlstrom, “Aeroelastic FE Modeling of Wind Turbine Dynamics”, Doctoral Thesis from Royal Institute of Technology Department of Mechanics, Sweden, 2005.

[4] J. M. Jonkman, P. D. Sclavounos, “Development of Fully Coupled Aeroelastic and Hydrodynamic Models for Offshore Wind Turbines”, ASME Wind Energy Symposium, 2006.

[5] I. Dobrev, F. Massouh, “Fluid-structure interaction in the case of a wind turbine rotor”, 18th Congrès Français de Mécanique, 2007.

[6] D.H. Kim, Y.S. Kim, D.M. Kim, Y.H. Kim and S.H. Kim, “Coupled Aeroelastic Analysis of a 3D Wind Turbine Blade Considering Rotating Flow Separation Effects:, 9th World Wind Energy Conference, 2009.

[7] Y.H. Kim, D.H. Kim, Y.S. Kim, S.H. Kim, “Comparison Study of Viscous Flutter Boundary for the AGARD 445.6 Wind Using Different Turbulent Boundary Layer Models”, The Korean Society of Mechanical Engineers, 2009.

[8] D.H. Kim, H.J. Kwon and I. Lee, "Transonic Aeroelastic Computations for a Full Configuration Fighter with Control Surface Motions and External Stores”, International Forum on Aeroelasticity and Structural Dynamics (IFASD) 2003, Amsterdam, The Netherlands, June 4-6, 2003.